**Mat. Res. Soc. Symp. Proc. Vol. 539, 1999, pp. 277-290**

# QUANTITATIVE MODELING AND MEASUREMENT OF COPPER THIN FILM ADHESION

A.A. VOLINSKY, N.I. TYMIAK, M.D. KRIESE, W.W. GERBERICH* and J.W. HUTCHINSON**
*University of Minnesota, Dept. of Chem. Engineering and Materials Science, Minneapolis, MN
** Harvard University, Division of Engineering and Applied Sciences, Cambridge, MA

## ABSTRACT

Numerous mechanisms have been identified as fundamental to the adhesion of thin metallic films. The primary mechanism is the thermodynamic work of adhesion of the interface, which in its most basic description is the difference between the surface energies of the two materials and that of the interface. This quantity is often described as leveraging the contributions of other mechanisms. One of the more important mechanisms is that of plasticity occurring in a process zone in the vicinity of the delamination boundary. A quantitative model to characterize the contributions of plastic energy dissipation has been developed and used to rationalize experimental adhesion assessments. This model incorporates the functional dependence of the film thickness and constitutive properties. Orders of magnitude increases in the practical work of adhesion were both observed and predicted. Experimentally, the films used for model comparison were sputter-deposited copper ranging from 40 to 3300 nm in thickness, with and without a thin 10 nm Ti underlayer. Nanoindentation induced delamination of the Cu from $SiO_2$/Si wafers were evaluated in the context of composite laminate theory to determine adhesion energies ranging from 0.6 to 100 J/m$^2$ for bare Cu and from 4 to 110 J/m$^2$ for Cu with the Ti underlayer.

## INTRODUCTION

Reliability of electronic devices that contain multi-layer thin films is strongly dependent on interfacial adhesion. Even if the film meets the design criteria in terms of its properties, failure to adhere to the substrate will cause a device failure. In many cases, elastic-plastic properties of a film are significantly different from those of a substrate. Extensive plastic deformation is likely to develop in the softer material before delamination is induced during an adhesion assessment test. This imposes restriction on the application of elastic methods of analysis. Elastic-plastic approaches for a hard film on a plastically deforming substrate has recently been developed [1,2] providing a basis for the experimental adhesion assessment. In contrast, while theoretical treatments for composites consisting of a ductile film sandwiched between two brittle materials are available [3,4], methods applicable for practical adhesion testing are still in the developing stages.

Ductile metal film-brittle dielectric substrate systems are of practical importance in microelectronics applications. It applies e.g. to copper as a new interconnect material. Opposite to Al, Cu adheres poorly to most dielectrics. For practical purposes adhesion is the total irreversible energy required to debond a thin film from a substrate. There are several contributing factors to the work of adhesion, thermodynamic (true) work of adhesion being the primary basis. In the present study we report the influence of another important contribution to the practical work of adhesion, that being the plastic energy dissipation in a ductile thin film. Changing the film thickness can vary the amount of plasticity. A simple plastic strip model as an upper bound for estimating plastic energy dissipation at the interfacial crack tip [5], is given by:

$$G = h\frac{\sigma_{ys}^2}{E}\left\{\ln\left[\frac{h}{b}\right]-1\right\} \qquad (1),$$

where h is the film thickness, E is the Young's modulus, $\sigma_{ys}$ is the yield stress, and b is the Burgers vector. In this model the plastic zone extends through the whole film thickness, and the Burgers vector is a cut-off. Note that this is slightly larger but of a similar form to that derived elsewhere from small scale yielding considerations [1]. Even though the yield stress of copper thin films measured by nanoindentation was shown to decrease with increasing film thickness [5], higher strain energy release rate values are expected for thicker ductile films [6,7] as the thickness increase dominates.

Adhesion of a Cu thin film can also be improved by putting a thin "glue" layer of another material between Cu and a dielectric substrate. Here a thin Ti underlayer was used to improve Cu film adhesion to $SiO_2$, thus increasing the amount of plastic deformation in Cu films.

## EXPERIMENT

### Thin film deposition

All thin film processing was conducted in a clean room environment. Silicon <100> wafers (100 mm in diameter, 0.5 mm thick) were thermally oxidized at 1100 °C in steam to grow 1.5 μm of $SiO_2$. Oxide thickness was measured with a Nanoscope Ellipsometer. Cu films from 40 nm to 3 μm thick were deposited in a 2400 Perkin-Elmer sputtering apparatus. During sputtering the base pressure of the system was 1 μTorr, and the Ar pressure was 12 mTorr. Substrate table rotation was used to achieve uniform Cu film thickness and nanostructure. The maximum temperature during film deposition reached 100 °C after which the system was cooled for one hour without breaking the vacuum in order to prevent film oxidation. Using a DEKTAK surface profiler, film thickness was measured and confirmed by RBS measurements. Some Cu films were sputtered over a 10 nm thick Ti "glue" layer on top of $SiO_2$. Residual stresses in Cu films were measured by the wafer curvature technique employing Stoney's equation [8], and ranged from 200 to 300 MPa tension. After all Cu films were deposited, a superlayer of 1.1 μm of W with 200-300 MPa compressive residual stress was sputtered over all Cu films in one run. Deposition parameters for the different layers are summarized in Table I.

Table I. Sputtering deposition parameters.

| Sputtered Material | Base Pressure, μTorr | Ar Pressure/Flow, mTorr/cm$^3$ min$^{-1}$ | Presputter time, min | Sputter power, W | Table rotation, rpm |
|---|---|---|---|---|---|
| Ti | 1 | 11/9.6 | 15 | 1000 | 3.8 |
| Cu | 1 | 12/12 | 15 | 1000 | 2 |
| W | 1 | 7.4/7 | 15 | 1000 | 3.8 |

### Superlayer indentation

A superlayer indentation method developed by Kriese, et al [9] was used for Cu thin film adhesion determinations. In the case of ductile or strongly adhered films it is often impossible to cause film delamination from the substrate by means of indentation. Ductile thin films cannot store enough strain energy necessary for crack initiation/propagation. Deposition of a hard film, capable of storing sufficient amounts of elastic energy over the film of interest, can result in multilayer debonding [10], producing bigger delamination radii (Figure 1). It also acts like a capping layer, preventing plastic flow of the underlying film in the vertical direction, adding normal stresses at the interfacial crack tip [3].

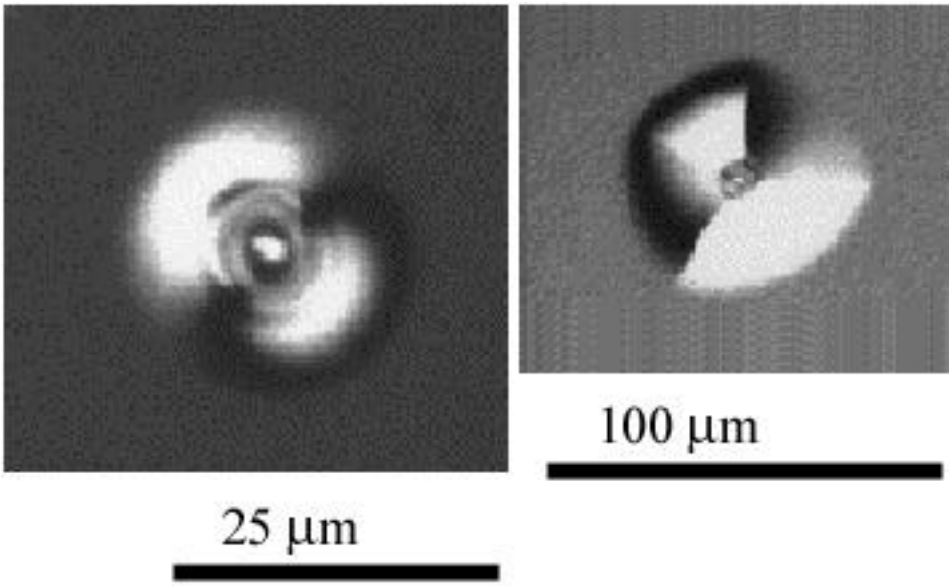


Figure 1. Optical micrographs of delaminations produced after indenting to 250 mN of load without and with a tungsten superlayer (420 MPa residual tensile stress) on Cu: Note the factor of four difference in scale.

In the superlayer test developed by Bagchi, et al high residual stress in the superlayer provides the driving force for film delamination [9]. Since residual stress is related to the superlayer thickness, several superlayer deposition steps are necessary for upper and lower bound adhesion assessment. For the superlayer indentation test a sharp indenter provides enough additional stress for crack initiation/propagation. As opposed to the Bagchi design, the sign of the residual stress in the superlayer does not have much effect on the interface cracking. Indentation stresses will overcome the residual tensile stress, or will be added to the compressive stress, promoting blister formation in both cases [5,3,11]. This makes the superlayer indentation test more versatile and easy to perform in terms of superlayer deposition and sample preparation. Superlayer indentation is schematically shown in Figure 2.

If the cracked film radius reaches the critical double-buckling conditions during loading, it will buckle. Upon the tip removal single buckling is also an option if the appropriate critical conditions are reached. Mechanics of the superlayer indentation test [9] is an extension of single layer Marshall and Evans analysis [12], and treats a bilayer as a single layer from the standpoint of laminate theory.

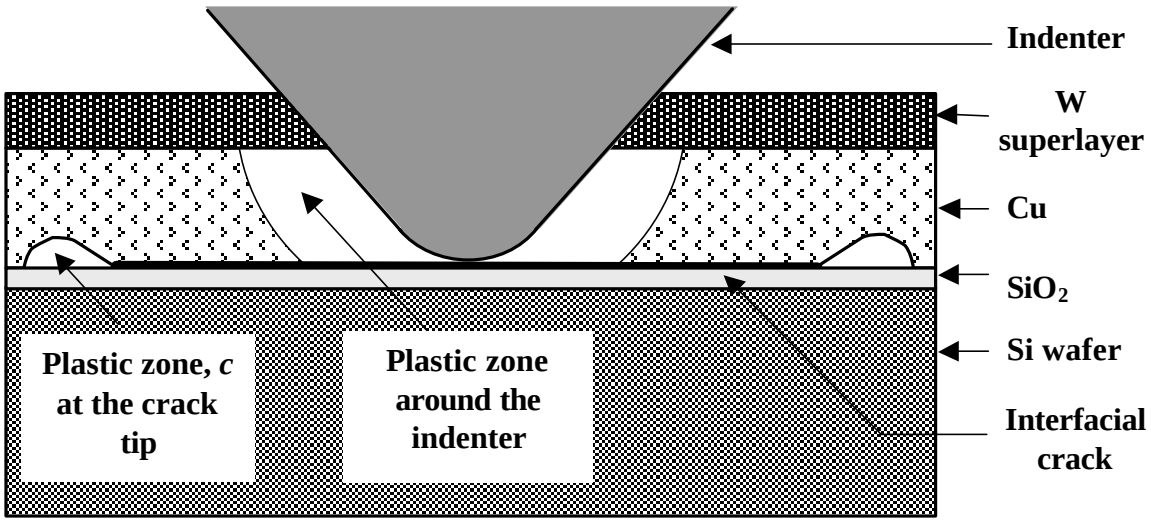


Figure 2. Superlayer indentation schematic.

**Fracture toughness assessment**

When an indenter penetrates through a bilayer, it causes film debonding and blister formation, which can be seen afterwards in an optical microscope with Nomarski contrast. Properties of the films such as elastic modulus, Poisson's ratio, as well as the tip angle and radius are needed for an adhesion assessment. Generally speaking, there are two measurements that are necessary for strain energy release rate calculations. From the standpoint of blister formation, both indentation depth and blister diameter are required. Blister diameter is measured in the optical microscope with Nomarski contrast, examples being presented in Figure 1. An Olympus optical microscope was calibrated for 50 and 100X magnifications prior to blister diameter measurement with a Tencor surface profilometer being used to verify the measurement accuracy.

Displacement controlled indentation tests were conducted using the IBM micromechanical tester described elsewhere [9,13]. A series of indents to maximum loads ranging from 30 to 250 mN were made with a conical 90° diamond indenter of 1 μm tip radius. Using the Oliver-Pharr method [14], indentation volume has been calculated from the indentation depth, as obtained by fitting 65% of the unloading portion of the load-displacement curve.

Besides plastic deformation, there are several other energy dissipation mechanisms for superlayer indentation. Friction between the film and the substrate behind the crack front may screen the crack tip from the applied load [15]. However, frictional effects are not considered in the present model. Cracking of the multilayer, as well as the substrate also releases strain energy, and is indirectly accounted for in the strain energy release rate calculations.

**Radial multilayer cracking**

For most of the indents into Cu films without a Ti underlayer, load excursions on the load-displacement curves were observed (Figure 3).

Discontinuities on the indentation curve can be attributed to multilayer buckling, unstable crack growth, radial multilayer cracking and substrate cracking. Since the indentation volume is calculated from the residual depth, it will be overestimated for indentations with load excursions,

which would result in the lower values for the calculated interfacial adhesion strength. Though the exact nature of excursions is not clear yet, it was accounted for in the analysis by subtracting the amount of excursions from the residual indentation depth. For shallower indentations, usually no radial cracking or load excursions were observed (e.g. indentation 1 in Figure 3). Increasing the indentation depth caused larger delamination radii, followed with a reproducible load excursion at 120-120 mN for a 100 nm thick Cu film. From this example it appears that the radial multilayer cracking contributes to discontinuities on the load-displacement curves. On the other hand, some curvature of Cu/W due to residual stress mismatch or double buckling could lead to a rapid interfacial crack advance followed by radial cracking.

The extent of radial cracks is highly dependent on the residual stress in the W superlayer. Tensile circumferential stress $\sigma_\theta$ in the delaminated film drives radial cracks initiated at the edge of the contact with an indenter. For a film with the residual compressive stress, $\sigma_\theta$ becomes compressive at the edge of a delamination while with the tensile residual stresses, $\sigma_\theta$ is always tensile. As reported in [4] for residual compressive stress, the indenter will produce radial cracks in the brittle film (W with 300 MPa compressive residual stress in this case) only up to a half of the delamination radius. This is clearly seen in Figure 3, indentation 2. In the case of tensile residual stress in W superlayer [9], radial cracks extend to the delamination radius (Figure 1).

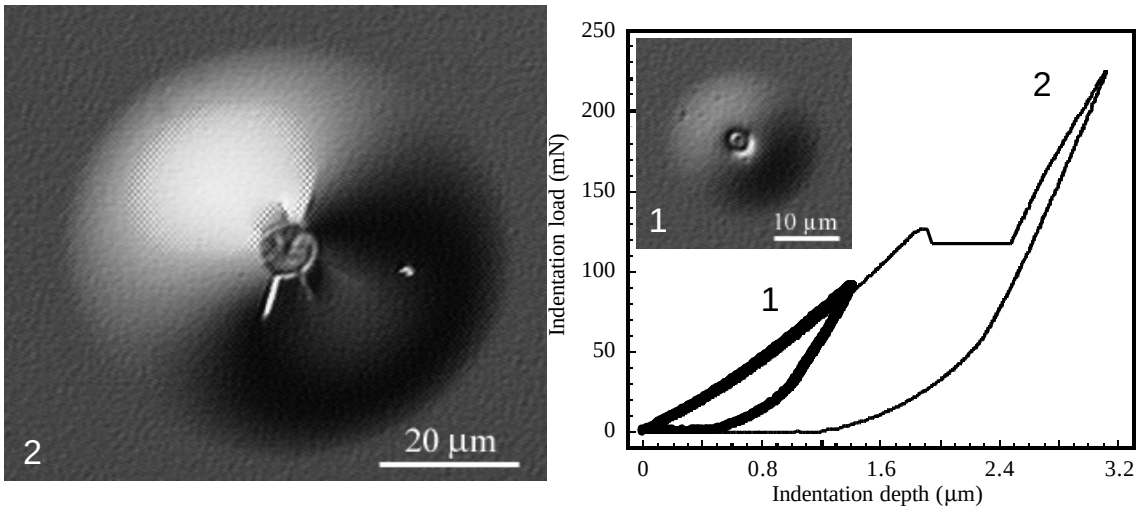


Figure 3. Load-displacement curves and corresponding delaminations for a 100 nm thick Cu film without Ti underlayer.

**Ti underlayer**

There are several reasons why a thin underlayer is necessary in the case of Cu films. From the standpoint of microelectronics, copper diffuses into silicon, reaching active devices. The underlayer is desirable to prevent copper diffusion. On the other hand, any additions to copper reduce film conductivity. The underlayer material is presumably nonreactive and nonmiscible with copper, should react with Si at high temperatures but not weaken copper electromigration properties. The underlayer is supposed to improve adhesion properties and thus improve mechanical reliability.

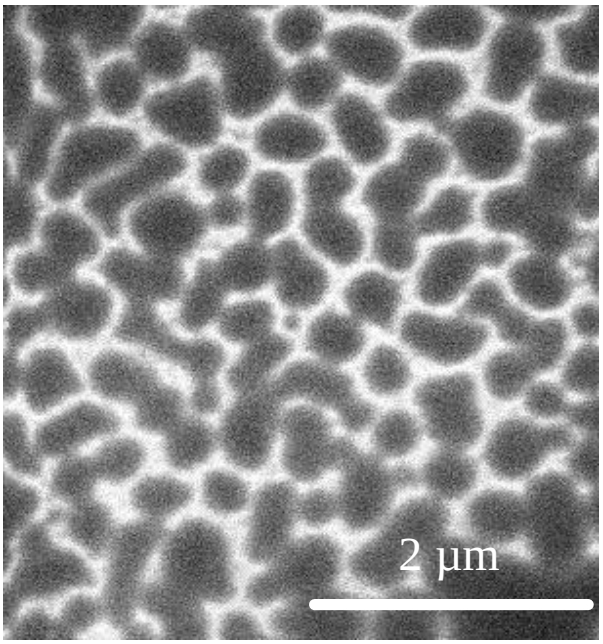


For the current study a thin (10 nm) layer of Ti was used to improve Cu film adhesion to silicon/silica substrates. There are two main reasons why Ti improves Cu adhesion in this case. First, there are two new interfaces that are formed, which are stronger than the original $SiO_2$/Cu one [16]. Second, being in its initial stage of island growth, the Ti film has higher surface roughness than $SiO_2$ (which simply increases the contact area between Ti and Cu). Since the vacuum was broken prior to Cu film deposition, $TiO_2$ oxide was most likely formed [17]. Thus, whatever increase in adhesion results must be considered either in terms of roughness or bonding to the titania.

Figure 4. SEM image of Ti underlayer.

**RESULTS AND DISCUSSION**

Interfacial fracture toughness values of Cu films are compiled in Figure 5. The plane strain solution for a wedge from [11] is presented for comparison. Elevated values for strain energy release rate are expected for the delamination radius to contact radius ratios up to five.

There are two components that contribute to the elastic energy in the film that drives interfacial delamination: indenter-induced stress and residual stress in the bilayer. For smaller delamination radii (R/a < 5 in case of a superlayer) there is an indenter-induced stress that drives the crack. For radii ratios over five the residual stress in the superlayer is mostly contributing to the annular crack growth.

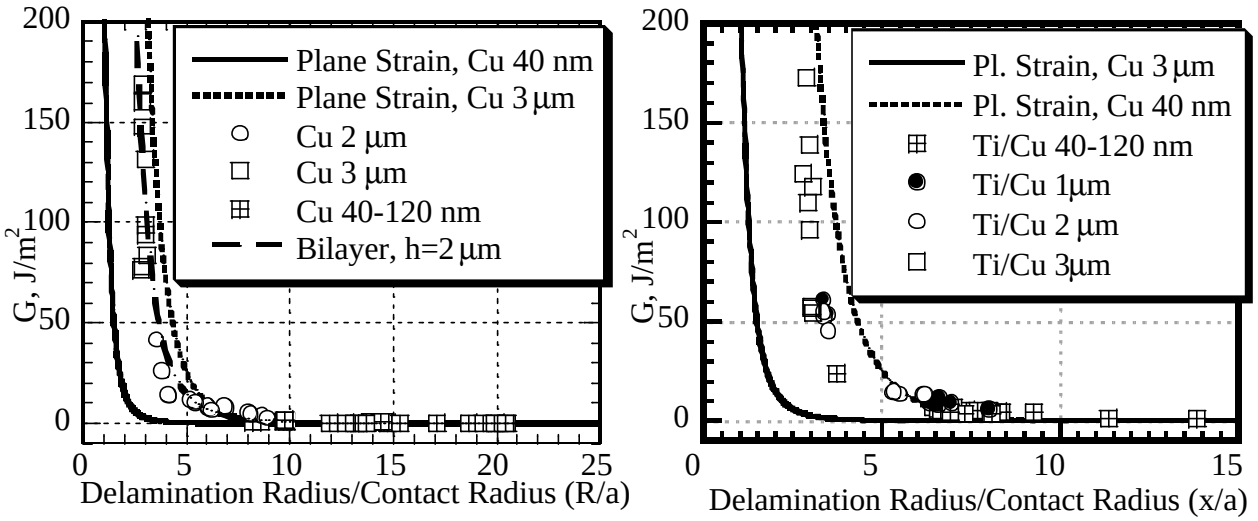


Figure 5. Strain energy release rate as a function of normalized delamination radius for Cu films a) without and b) with Ti underlayer.

The bi-layer solution for a 2 μm thick Cu film is also presented. This solution is constructed by fixing the indentation depth at 0.64 of the bilayer thickness and varying the delamination radius. For a given indentation depth and bilayer thickness there will be a unique

curve. Both plane strain and bilayer solutions show that for thicker films higher strain energy release rate values are expected for a given R/a ratio. For R/a < 5, variations in the delamination radius as measured optically will produce significant changes in the measured adhesion. Note that for a given load, bi-layer blisters without Ti are much larger compared to those with the Ti underlayer, as shown in Figure 6a. Corresponding indentation curves are shown in Figure 6b.

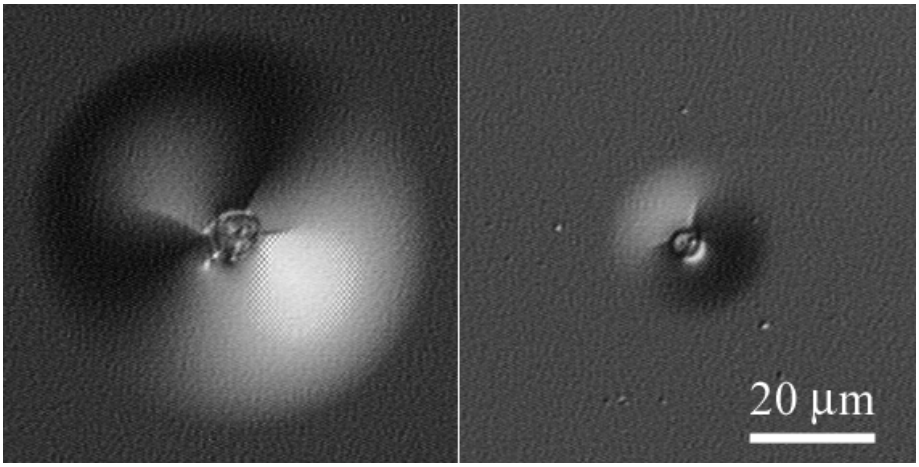


Figure 6a. Indentation induced delaminations in a 100 nm Cu film with and without Ti underlayer.

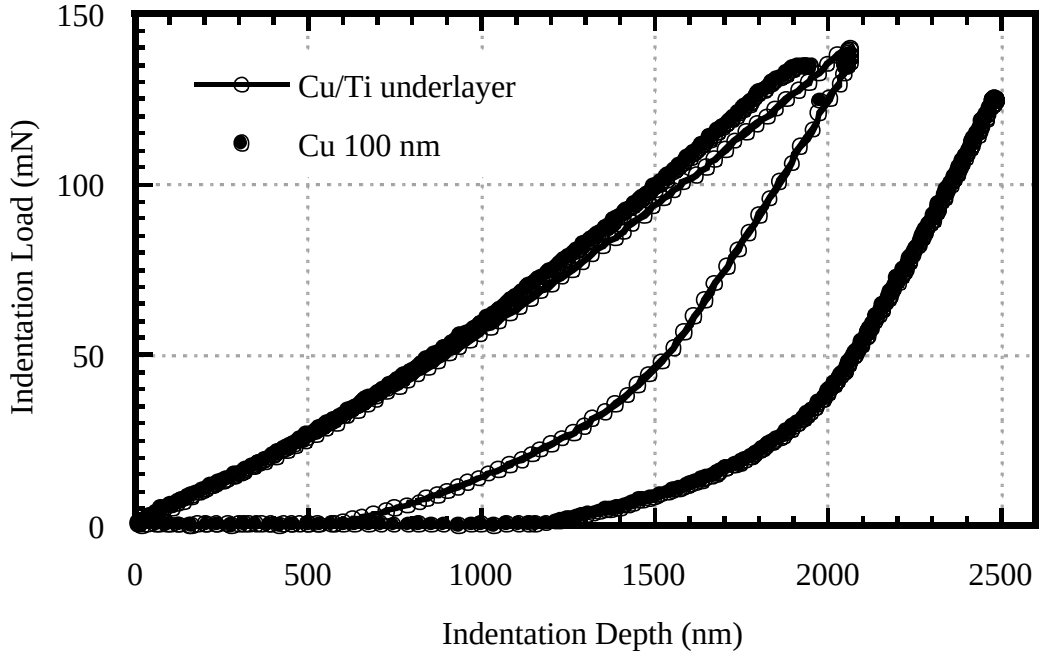


Figure 6b. Load-displacement curves corresponding to delaminations in Figure 6a.

For Cu films with a Ti underlayer, R/a ratios do not exceed 15, compared to 21 without Ti. Improved Cu adhesion in the case of Ti underlayer does not allow blister extensions over R/a ratios higher than 15. Indenting deeper than the bilayer thickness into the substrate does not increase the blister size substantially, but causes substrate cracking and invalidates the analysis.

Residual stresses in Cu and W layers both affect G values. While W stresses were the

same for both films with and without Ti, residual tension was slightly higher for the Cu/Ti films as shown in Figure 7.

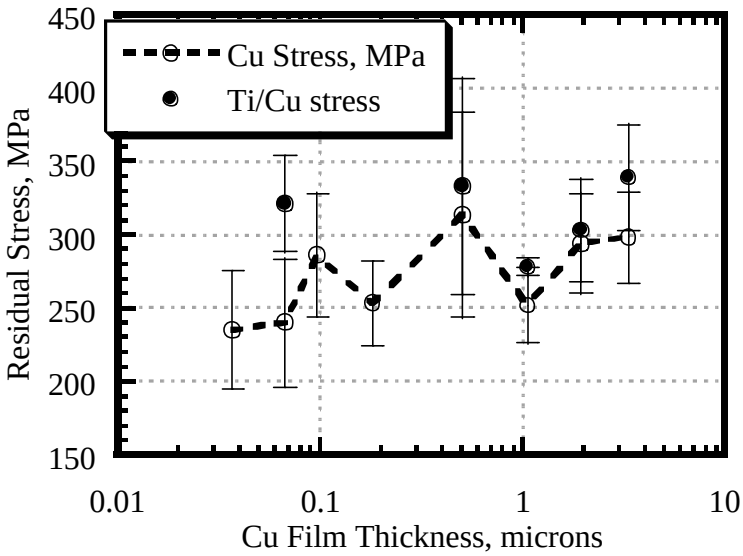


Figure 7. Residual stress levels in the Cu and Ti/Cu films.

A higher tensile stress in Cu layer would result in increased curvature of the delaminated Cu/W. Thus, with the Ti underlayer, the crack tip would be more heavily under Mode I conditions. In fact, this prediction is consistent with the phase angle estimates as will be shown later. A shift towards Mode I would decrease measured adhesion strength, opposite to experimental observations as shown in Figure 8. Overall, the strain energy release rate is higher for films with this underlayer for a given film thickness. Here, the plastic energy dissipation upper bound estimate as given by equation (1) is also presented for comparison. This estimate assumes the plastic zone size extends through the entire film thickness. While being in qualitatively good agreement with the experimental results, the model is clearly an overestimate. One of the possible reasons could be the assumption that the plastic zone extends through the entire film thickness. Thus, it was desirable to estimate plastic zone size based on the experimentally measured strain energy release rates.

**Plastic zone size at the crack tip**

If the fracture toughness of the interface is known, a plastic strip model described in [5] can be used for estimating plastic zone size, *c* at the crack tip. Similar assumptions are considered here:

1) Elastic-perfectly plastic material;
2) No contribution from substrate or superlayer;
3) Use Burgers vector, b as a cut-off;
4) The average stress is equal to the yield stress of the film.

The difference here is that the plastic zone does not necessarily extend to the film thickness, but to some finite distance c < h. Work per unit fracture area can be determined as follows:

$$G = \frac{dW}{dA} = \frac{\int \sigma \, d\varepsilon \cdot dV}{dA} = c \int \sigma \, d\varepsilon \approx c \, \sigma_{ys} \frac{1}{c-b} \int_b^c \varepsilon(r) \, dr \qquad (2),$$

where c is a finite plastic zone size, b is Burgers vector, $\varepsilon(r)$ is the plastic strain at a distance r from the crack tip, as given by [18]:

$$\varepsilon(r) = \frac{\sigma_{ys}}{E} \cdot \left( \frac{c}{r} - 1 \right) \tag{3}$$

Substituting (3) into (2) and integrating yields:

$$G = c \frac{\sigma_{ys}^2}{E} \left\{ \ln\left[\frac{c}{b}\right] - 1 + \frac{b}{c} \right\} \approx c \frac{\sigma_{ys}^2}{E} \left\{ \ln\left[\frac{c}{b}\right] - 1 \right\} \tag{4}$$

Since the plastic zone, c is still much bigger than the Burgers vector, the last b/c term can be omitted in this case except perhaps for very small thicknesses. Note that (4) reduces to (1) at the upper bound where c = h. If G is known, equation (4) can be solved for c numerically. Results of the crack tip plastic zone size calculations are presented in Figure 9.

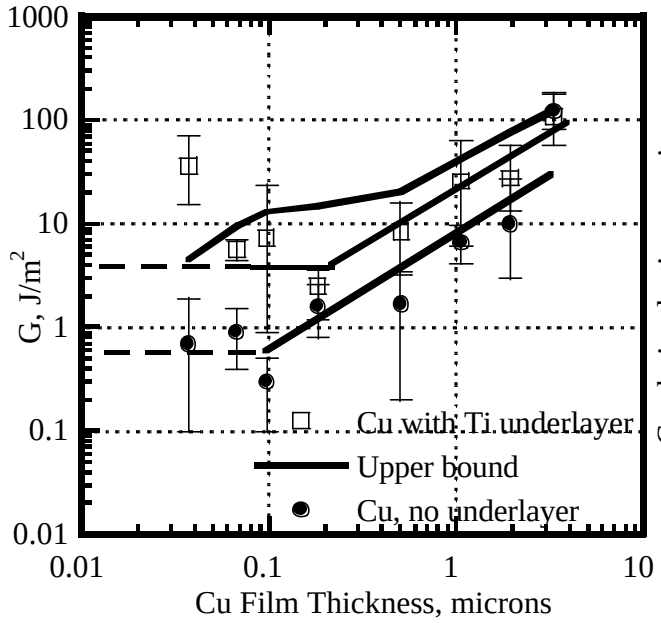


Figure 8. An interfacial energy relationship to the film thickness: theoretical upper bound solution (top solid line) and experimental strain energy release rates. Note: error bars span the full range of data, from 9 to 16 points.

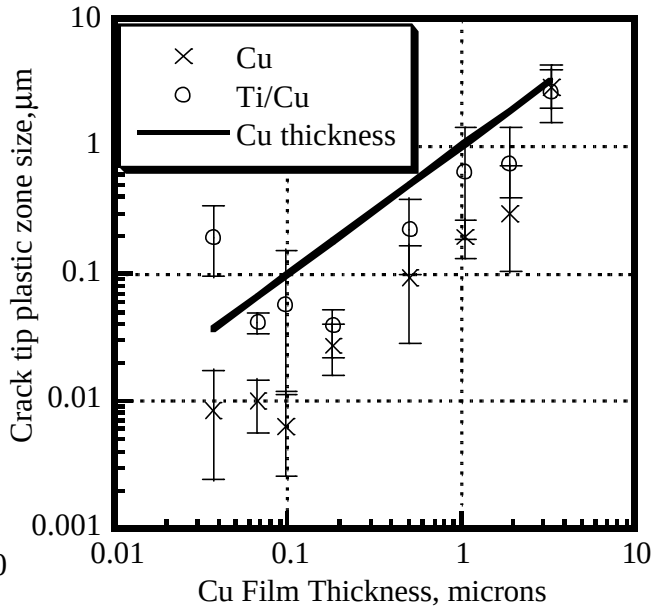


Figure 9. Crack tip plastic zone for Cu films without Ti underlayer. Calculations from the modified plastic strip model, equation (4)

Here, it is seen that the plastic zone size is always larger with the Ti underlayer, and is approaching the film thickness. Since the Cu film adhesion was higher in this case, much more energy was spent on Cu film plastic deformation, approaching the upper bound of Figure 9.

Since measured interfacial fracture toughness is strongly dependent on the mode mixity, estimate of phase angle variations with the changing Cu/W film thickness ratio is desirable. This would assist in sorting whether the improved adhesion was solely due to plastic energy dissipation as opposed to contributions from a change in phase angle.

**Phase angle determination**

To obtain an estimate of phase angle, a procedure originally defined elsewhere [5] but not completely derived is used here. First, for Mode I conditions the values of $G_0$, an initiation strain energy, can be taken from Mao, et al [19, 5] for pure Mode I loading to be

$$G_0=\left(\frac{\pi}{8}\right)\frac{\sigma_b^2\Delta}{E} \tag{5}$$

where $\sigma_b$ is the interfacial bond strength, $\Delta$ is the crack blunting distance, and E is Young's modulus. The number of dislocations piled-up at a boundary may be given by $N=\Delta/b$ with N further defined in terms of the shear stress acting on the boundary [20], giving

$$N=\frac{\Delta}{b}\approx\frac{\tau_i d}{2A^*} \tag{6}$$

with $A^* = \mu b/2\pi(1-\nu)$; d, the pile-up length; $\mu$, as the shear modulus; $\nu$ , Poisson's ratio. To first order we take $\tau_i$ to be associated with the maximum shear stress. Since the shear stress at initiation is largely elastic as governed by the preponderance of tungsten in most cases, this becomes

$$\tau_i \approx \tau_{max} \approx 0.3p_0 = 0.45\frac{P}{\pi a^2} \tag{7},$$

where $p_0$ is the maximum pressure or 3/2 the mean pressure, P is load and a is the contact radius. Since the $P/\pi a^2$ in (7) is hardness ,H, the number of dislocations of interest from (5)-(7) becomes

$$N=\frac{Hh}{\mu b} \tag{8}$$

with the pile-up length, d, being taken as the film thickness, h. Further, taking hardness to be three times the yield strength, $\sigma_{ys}$ , it is easily shown with (5)-(8) that

$$G_0 \approx \frac{3\pi}{8}\frac{\sigma_b^2\sigma_{ys}h}{E\mu} \tag{9}$$

It is seen that by measuring $G_0$ we can estimate bond strength since $\sigma_{ys}$, h, E and $\mu$ are known. Furthermore, as discussed elsewhere [5], we can estimate the tangential shear stress from elasticity theory and therefore estimate a phase angle from

$$\psi' = \tan^{-1}\left(\frac{\tau_r}{\sigma_b}\right) \tag{10}$$

First, the ratio of $\tau/\sigma_b$ is determined using experimentally measured values of $G_0$. Converting this to a phase angle through equation (10) gives the phase angle versus normalized film thickness in Figure 10a.

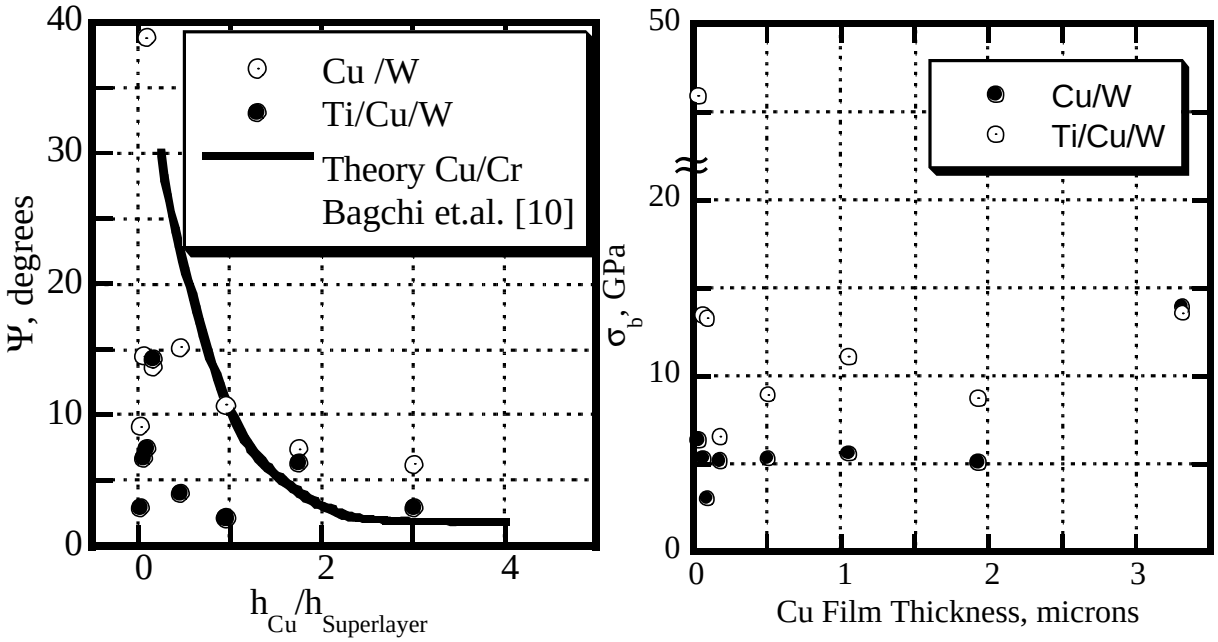


Figure 10a. Phase angle. b. Bond strength.

The phase angle decreases quite rapidly from about 20 degrees to 5 degrees with increasing Cu thickness compared to the superlayer. This trend is consistent with the theoretical predictions presented in the Appendix. The important point is that the material with the titanium underlayer has a slightly lower measured phase angle. This indicates a smaller Mode II component being involved in the delamination process. Since a smaller mode II component should result in a decreased strain energy release rate, the obvious conclusion is that the mode II component is not a controlling factor here. On the other hand, presence of the Ti underlayer results in approximately doubling in the true adhesion strength as shown in Figure 10b. Here, bond strengths for Ti/Cu/W and Cu/W films are given by equation (5). Note that estimated values are nearly independent of the film thickness for both types of multilayers. It may be concluded that the increased strain energy release rate observed in Figure 8 with the Ti underlayer cannot be attributed to a phase angle effect. The conclusion, using an admittedly first order calculation of a true bond strength and phase angle, is that the important contribution of the Ti is improved bonding and therefore an increased plastic energy dissipation.

**Practical and true works of adhesion**

Regarding the present adhesion measurements, there are three important points we wish to make here:

i) Cu films both with and without a Ti underlayer have increased interfacial energy release rates with increasing thickness;

ii) a Ti underlayer increases both interfacial toughness and interfacial bond strength, but the later is independent of film thickness;

iii) on both theoretical and experimental grounds, the phase angle decreases with an increasing ductile layer thickness, in this case Cu.

These three points taken together are consistent with plastic energy dissipation in the Cu films being the primary contributor to improved adhesion energies. While a Mode II contribution might be a minor factor in all cases but one, the calculated phase angle, $\psi = 15°$ is sufficiently small to reinforce the proposed concept that plastic zone sizes are generally about a factor of two smaller than the Cu film thickness implying that an even stronger bonding agent might further improve interfacial fracture toughness. The one disturbing feature about the data with the Ti underlayer is that strain energy release rate appears to increase with decreasing Cu film thickness below about 100 nm. Presently it is not known whether this is an artifact in our calculated values where R/a is quite small (see Figure 5b) or whether some Ti/Cu intermixing at very small Cu thicknesses allows improved bonding to the W superlayer resulting in nonlinear dissipation contributions from the tungsten. It is also possible that the above trends can possibly be attributed to the interfacial friction producing screening of a crack tip from the applied load. As follows from Stringfellow and Freund's [15] theoretical results, screening effects should be negligible at higher film thicknesses but increase with decreasing film thickness. Higher surface roughness of Ti as compared to $SiO_2$ could possibly result in more effective screening of a crack tip from the applied load. Thus, adhesion strength of Cu films thinner than 100 nm could be increased via interfacial friction when Ti is present but remain unaffected for the films with no Ti. In fact, we wish to point out that the Cu only films behave in an orderly fashion with a plateau of $G = 0.6$ J/m$^2$ for thicknesses less than or equal to 100 nm. This translates to a stress intensity factor of 0.27 MPa$\cdot$m$^{1/2}$. Using the yield strength for 120 nm thick film, and $\sigma_{ys} \cong 1.86$ GPa from a deconvolution program, one finds a plane strain plastic zone of only 22 Å. Since this is practically the stand off distance for a single dislocation (Burgers vector), it can be assumed that plastic energy dissipation is nil. As pointed out elsewhere, [6], the stress intensity factor of 0.27 MPa$\cdot$m$^{1/2}$ is only slightly less than Rice and Thompson's estimate for dislocation emission in Cu, $k_{Ie}$=0.32 MPa $\cdot$ m$^{1/2}$. Taken together, it would appear that we have measured at the plateau, the true work of adhesion, i.e. the thermodynamic value of fundamental interest.

## SUMMARY AND CONCLUSIONS

Plastic energy dissipation effects on the toughness of a thin ductile film/brittle substrate interface have been quantitatively evaluated. Predictions of a proposed theoretical model have been compared to the experimental results for Cu/$SiO_2$ interface with and without a Ti underlayer. Experimental adhesion strength assessment relied on the superlayer indentation technique and axisymmetric bi-layer theory. Values ranging from 0.6 to 100 J/m$^2$ and from 4 to 110 J/m$^2$ increasing with the film thickness were obtained for Cu/$SiO_2$ and Cu/Ti/$SiO_2$ systems, respectively. Observed trends in interfacial toughness vs. film thickness dependencies were in qualitatively good agreement with the theoretical model. Bond strength estimates yielded average values of 10 GPa and 5 GPa for films with and without Ti underlayer, respectively. These values were nearly constant through all the range of Cu layer thicknesses indicating a *true adhesion strength* independent of the film thickness. Estimated phase angle values respectively ranged from 6 to 40° and from 2 to 14° for Cu/$SiO_2$ and Cu/Ti/$SiO_2$ systems. In both cases, increasing Cu film thickness resulted in a shift towards Mode I conditions. For the entire range of Cu film thicknesses,

estimated plastic zone sizes were higher with the presence of Ti underlayers as compared to the films with no underlayer.

Taking into account the above, plastic energy dissipation has been identified as the mechanism primarily responsible for the observed elevation of the interfacial fracture toughness.

## ACKNOWLEDGMENTS

The authors would like to acknowledge support for this work by the Center for Interfacial Engineering at the University of Minnesota under grant NSF/CDR-8721551, the Department of Energy under DOE contract DE-FG02/96ER45574. In addition, N.I.T. wishes to thank Prof. J.V.R. Heberlein and Prof. S.L. Girshick of the University of Minnesota for support under NSF DMI-9871863. The assistance of Dr. J.C. Nelson from the Center for Interfacial Engineering and Microtechnology Laboratory staff at the University of Minnesota is also gratefully appreciated.

## REFERENCES

1. Y. Wei and J.W. Hutchinson, J.Mech.Phys.Solids, (1997), **45,** pp. 1137-1159
2. M.D. Drory and J.W. Hutchinson, Proc. R. Soc. Lond. A. (1996) **452**, pp. 2319-2341
3. M.Y. He, A.G. Evans and J.W. Hutchinson, Acta Metall. Mater., 1996, Vol. 44, pp. 2963-71
4. V. Tvergaard, J.W. Hutchinson, J.Mech.Phys.Solids, (1996), **44,** pp. 789-800
5. N.I. Tymiak, A.A. Volinsky, M.D. Kriese, S.A. Downs and W.W. Gerberich, submitted to Metallurgical Transactions, 1998
6. W.W. Gerberich, D.E. Kramer, N.I. Tymiak, A.A. Volinsky, D.F. Bahr and M.D. Kriese,submitted to Acta Metall. Mater., 1998
7. R.H. Dauskardt, M. Lane, Q. Ma, Submitted to Engineeing Fracture Mechanics, 1997
8. G.G. Stoney,Proc.Roy.Soc.Lond. **A82** (1909) p.72
9. M.D. Kriese, N.R. Moody and W.W. Gerberich, Acta Metall., 1998
10. A. Bagchi and A. G. Evans, Thin Solid Films, (1986), **286**, pp. 203-12
11. J.J. Vlassak, M.D. Drory and W.D. Nix, J. Mater. Res., (1997), **12**, No 7, p. 1900-10
12. D.B. Marshall and A.G. Evans, J. Appl. Phys., 1984, **56**, pp. 2632-38
13. T. Wu, J. Mater. Res., (1991), **6** No. 2, pp. 407-426
14. W.C. Oliver and G.M. Pharr, J. Mater. Res., **7**, (1992), pp.1564-1583
15. R.G. Stringfellow and L.B. Freund, Int.J.Solids Structures, **30** (1993), **239**, pp. 1379-1395
16. Y. Shacham-Diamand, A. Dedhia, D. Hoffstetter and W.G. Oldham, J. Electrochem. Soc., **140** (1993), p. 93
17. S.W. Russell, S.A. Raflaski, R.L. Spreitzer, J. Li, M. Moinpour, F. Moghadam, T.L. Alford, Thin Solid Films **262** (1995), pp. 154-167
18. F.A. McClintock and G.R. Irwin, Plasticity Aspects of Fracture Mechanics, Fracture Toughness Testing and its Applications, ASTM STP 381, Philadelphia, 1965, pp. 84-113
19. S.X. Mao and A.G. Evans, Acta Mater., **45** (1997), 4263-4270
20. A.T. Yokobori, T.Y. Yokobori and H. Nioshi, in Macro-and Micro-Mechanics of High Velocity Deformation and Fracture, IUTAM Symposium, Tokyo, 1985, Springer-Verlag, Berlin (1987)
21. J.W. Hutchinson, M.D. Thouless and E.G. Linger, Acta Metall.Mater., **40** (1992), pp. 295-308

## APPENDIX

Effects of film thickness and interfacial crack length on the mode mixity for buckling driven delamination in the indented pre-stressed film can be qualitatively evaluated through the parameter $\eta = \sigma/\sigma_c$. Here, $\sigma_c$ is the critical buckling stress; $\sigma = \sigma_i + \sigma_R$ is the total stress in the film with the $\sigma_i$ and $\sigma_R$ being indentation induced stress and residual film stress respectively. As $\eta$ increases, $|\psi|$ increases with the interface crack becoming more heavily under mode II conditions [21]. The parameter $\eta$ can be determined using values of $\sigma_i$ and $\sigma_R$ defined by the Marshall and Evans [12] analysis for a single layer, giving

$$\eta = \frac{\sigma_i + \sigma_R}{\sigma_c} = \frac{\sigma_R + \beta E V_0 / R^2 h}{\gamma E h^2 / R^2} = \frac{\sigma_R R^2 + \beta E V_0 / h}{\gamma E h^2} \qquad (A.1)$$

Here, $\gamma = 14.68/12(1-\nu^2)$; $\beta = 1/2\pi(1-\nu)$; $V_0$ is the indentation volume; $\nu$, Poisson's ratio; E, Young's modulus and compression is regarded as a positive stress. In the case of a bi-layer film, $\sigma_R$ should be replaced with the *effective* residual stress in the laminate. For the Cu/W thickness ratios and residual stress levels considered in the present research, the effective $\sigma_R$ is always positive.

Differentiating (A.1) with respect to the delamination radius yields:

$$\frac{\partial \eta}{\partial R} = \frac{2\sigma_R R}{\gamma E h^2} \qquad (A.2)$$

As follows from (A.2), $\eta$ increases with the delamination radius if the effective residual stress in the bi-layer is compressive. On the other hand, the derivative $\frac{\partial \eta}{\partial h}$ is always negative providing $s_R > 0$:

$$\frac{\partial \eta}{\partial h} = -\frac{1}{E\gamma}\left(2\sigma_R R^2 / h^3 + 3\beta E V_0 / h^4\right) \qquad (A.3)$$

Thus, mode mixity decreases with increasing film thickness, which is consistent with the experimental calculations.